

Spatial Concept-based Topometric Semantic Mapping for Hierarchical Path-planning from Speech Instructions

Akira Taniguchi¹, Shuya Ito¹, and Tadahiro Taniguchi¹

Abstract— Navigating to destinations using human speech instructions is an important task for autonomous mobile robots that operate in the real world. Spatial representations include a semantic level that represents an abstracted location category, a topological level that represents their connectivity, and a metric level that depends on the structure of the environment. The purpose of this study is to realize a hierarchical spatial representation using a topometric semantic map and planning efficient paths through human-robot interactions. We propose a novel probabilistic generative model, SpCoTMHP, that forms a topometric semantic map that adapts to the environment and leads to hierarchical path planning. We also developed approximate inference methods for path planning, where the levels of the hierarchy can influence each other. The proposed path planning method is theoretically supported by deriving a formulation based on *control as probabilistic inference*. The navigation experiment using human speech instruction shows that the proposed spatial concept-based hierarchical path planning improves the performance and reduces the calculation cost compared with conventional methods. Hierarchical spatial representation provides a mutually understandable form for humans and robots to render language-based navigation tasks feasible.

I. INTRODUCTION

It is important for autonomous robots that coexist with humans in the real world to accomplish linguistic interaction tasks, such as navigation. To fulfill this task, the robot must adaptively form spatial structures and place semantics from the multimodal observations obtained while moving in the environment [1], [2]. Topometric semantic maps are useful for path planning using the generalized units of place, human-robot linguistic interaction, and robot support for humans. How robots can efficiently construct and utilize such hierarchical spatial representations for interaction tasks is a major challenge. The main purpose of this study was to realize efficient spatial representations and high-speed path planning from human speech instructions using topological semantic maps based on transitions between places.

Hierarchical spatial representation provides a mutually understandable form for humans and robots to render language-based navigation tasks feasible. As shown in Fig. 1, this study deals with the following three levels of spatial representation. (i) The semantic level, which represents place categories

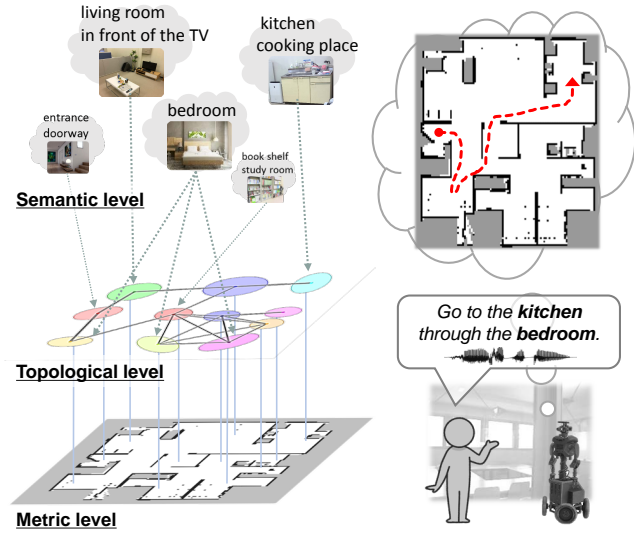


Fig. 1: Outline of this study. Left: Hierarchy of spatial representation with topometric semantic mapping; Right: Path planning from spoken instruction with the waypoint and goal.

associated with words and abstracted by multimodal observations; (ii) The topological level, which represents the adjacency of places in a graph structure; (iii) The metric level, which represents the occupied grid map was obtained by simultaneous localization and mapping (SLAM). In this study, semantic knowledge in a multimodal place category is termed a spatial concept. This study had two phases: spatial concept learning and path planning. In learning, we assumed a scenario in which a robot moves around the environment with a person, and the person speaks about the location. In path planning, we assume that the robot is given speech instructions, such as ‘*go to the kitchen*’ as a basic task and ‘*go to the kitchen through the bedroom*’ as an advanced task. In particular, this study focuses on hierarchical path planning.

SpCoSLAM [3] forms spatial concept-based semantic maps based on multimodal observations obtained from the environment. SpCoSLAM can acquire novel place categories and vocabularies from unknown environments. However, SpCoSLAM has not been able to estimate the adjacency and transition probabilities between places, that is, whether one place is spatially connected to another. In this study, we applied the hidden semi-Markov model (HSMM), which estimates the transition probabilities between places and constructs a topological graph. In addition, SpCoNavi [4] plans the path in the framework of *control as probabilistic*

*This work was partially supported by JST CREST under Grant number JPMJCR15E3, including the AIP Challenge Program, JST Moonshot Research & Development Program under Grant number JPMJMS2011, and JSPS KAKENHI under Grant numbers JP20K19900 and JP21H04904.

¹Akira Taniguchi, Shuya Ito, and Tadahiro Taniguchi are with Ritsumeikan University, 1-1-1 Noji-Higashi, Kusatsu, Shiga 525-8577, Japan. {a.taniguchi, ito.shuya, taniguchi}@em.ci.ritsumei.ac.jp

inference (CaI) [5], which focuses on the action decision in the probabilistic generative model of SpCoSLAM. SpCoNavi has realized navigation from simple speech instructions using a spatial concept acquired autonomously by the robot. However, there are some problems to be solved: The Viterbi algorithm is computationally expensive because all grids of the occupied grid map are used as the state space, and it is vulnerable to the real-time performance required for robot navigation. The A* approximation reduces the computational cost, but its performance is inferior to that of the Viterbi. Therefore, in this study, we utilized a topological semantic map based on spatial concepts to reduce the number of states and enable the rapid inference of possible paths to be traveled between each state. In addition, we applied it to the case of specifying the waypoint.

We propose a probabilistic generative model for spatial concept-based topometric semantic mapping for hierarchical path planning (SpCoTMHP)¹. The proposed topometric semantic map enables path planning that combines abstracted place transitions and geometrical structures in the environment. We also developed approximate inference methods for effective path planning, where each level of the hierarchy can influence the others. The proposed path planning is theoretically supported by deriving a formulation based on CaI. The main contributions of this work are as follows:

- 1) We propose an integrated model capable of both topometric semantic mapping and hierarchical path planning.
- 2) We show that the proposed method enables efficient path planning even with speech instructions that specify waypoints.

II. RELATED WORK

A. Topometric semantic map

In recent years, research on semantic mapping, which assigns a place to a robot's map [1], [2], has been emphasized. However, many existing studies provide a preset location label for an area on a map. Our approach allows unsupervised learning based on multimodal perceptual information for categorizing unknown places and flexible vocabulary assignments.

The use of topological structures enables more accurate semantic mapping [6]. Our method is also expected to improve its performance by introducing topological levels. The nodes in a topological map can vary depending on the method, such as room units or small regions [7], [8]. Kimera [9] used multiple levels of spatial hierarchical representation, such as metrics, rooms, places, semantic levels, objects, and agents. In our study, the robot automatically determined the spatial segmentation unit based on experience.

Some semantic mapping studies [10], [11] have successfully constructed topological semantic maps from visual images or metric maps using convolutional neural networks. However, these studies have not been demonstrated for path

¹The source code is available at <https://github.com/a-taniguchi/SpCoTMHP.git>.

planning. In contrast, our method is characterized by the integrated model being inclusive of learning and planning.

B. Hierarchical path planning

In terms of sampling candidate points and connecting them in planning, our method is related to a probabilistic roadmap (PRM) [12] and rapidly exploring a random tree (RRT) [13]. In contrast to PRM and RRT, which place waypoints completely randomly in space, our method allows the targeted sampling of promising candidates according to the destination named in the utterance.

Hierarchical path planning has long been a topic of study, as in hierarchical A* [14]. The use of topological maps for path planning (including the learning of paths between edges) is more effective for reducing computational complexity than considering only the movement between cells in a metric map [7], [9], [15]. In addition, the extension to semantic maps enables navigation based on speech [16].

Because our method realizes a hierarchy based on the CaI framework [5], it is theoretically connected with hierarchical reinforcement learning. In hierarchical reinforcement learning, sub-goals and policies are autonomously estimated [17], [18]. In our study, tasks similar to hierarchical reinforcement learning were realized to infer probabilistic models. In addition, recent studies on vision-and-language navigation have used deep and reinforcement learning [19], [20]. The proposed probabilistic model autonomously navigates toward the target location using the speech instructions as a modality.

III. PROPOSED METHOD: SPCoTMHP

We propose a spatial concept-based topometric semantic mapping for hierarchical path planning (SpCoTMHP). The proposed method realizes efficient navigation from human speech instructions through inference based on a probabilistic generative model. The capabilities of the proposed generative model are as follows: (i) Place categorization by extracting connection relations between places using unsupervised learning; (ii) Many-to-many correspondence between words and places; and (iii) Hierarchical path planning by introducing two types of variables with different time constants. The SpCoTMHP is designed as an integrated model for each module, as shown in Fig. 2. Therefore, it is easy to develop further module coupling in the Neuro-SERKET framework [21].

A. Definition of the probabilistic generative model

SpCoTMHP is an integrated SLAM model, a hidden semi-Markov model, a multimodal mixture model for place categorization (based on positions, speech-language, and image features), and a speech recognition model. Figure 2 shows the graphical model representation of SpCoTMHP for learning the global parameters, and Table I lists each variable of the graphical model. The details of the formulation of the generative process represented by the graphical model of

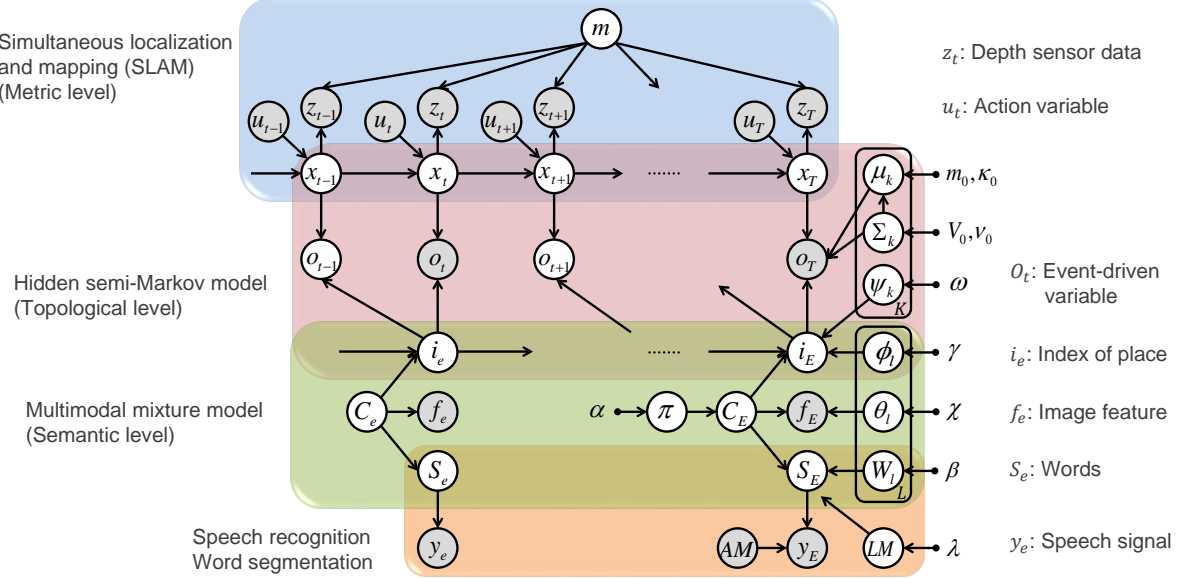


Fig. 2: Graphical model representation of SpCoTMHP for topometric spatial concept formation and hierarchical path planning. The graphical model represents the conditional dependency between random variables. Gray nodes indicate observations, and white nodes denote unobserved latent variables. Several arrows from the global variables to local variables other than T and E are omitted.

SpCoTMHP are as follows.

$$\begin{aligned}
 \pi &\sim \text{DP}(\alpha) & (1) \\
 \phi_l &\sim \text{DP}(\gamma) & l = 1, 2, \dots, \infty & (2) \\
 \theta_l &\sim \text{Dir}(\chi) & (3) \\
 W_l &\sim \text{Dir}(\beta) & (4) \\
 LM &\sim p(LM | \lambda) & (5) \\
 \psi_k &\sim \text{DP}(\omega) & k = 1, 2, \dots, \infty & (6) \\
 \Sigma_k &\sim \mathcal{IW}(V_0, \nu_0) & (7) \\
 \mu_k &\sim \mathcal{N}(m_0, \Sigma_k / \kappa_0) & (8) \\
 C_e &\sim \text{Mult}(\pi) & e = 1, 2, \dots, E & (9) \\
 f_e &\sim \text{Mult}(\theta_{C_e}) & (10) \\
 S_e &\sim p(S_e | C_e, W, LM) & (11) \\
 i_e &\sim p(i_e | C_e, \phi, \psi_{i_{e-1}}) & (12) \\
 y_e &\sim p(y_e | S_e, AM) & (13) \\
 x_t &\sim p(x_t | x_{t-1}, u_t) & t = 1, 2, \dots, T & (14) \\
 z_t &\sim p(z_t | x_t, m) & (15) \\
 o_t &\sim p(o_t | x_t, i_e, \mu, \Sigma) & t = t_e, \dots, t'_e & (16) \\
 D_e &\sim \text{Unif}(1, T) & t_e = \sum_{e' < e} D_{e'} & (17) \\
 & & t'_e = t_e + D_e - 1 & (18)
 \end{aligned}$$

where $\text{DP}()$ represents the Dirichlet process, $\text{Dir}()$ is the Dirichlet distribution, $\mathcal{IW}()$ is the inverse Wishart distribution, $\mathcal{N}()$ is a multivariate Gaussian distribution, and $\text{Mult}()$ is a multinomial distribution. The duration distribution assumes uniform distribution $\text{Unif}()$ in $[1, T]$.

Self-localization assumes a transition at time t owing to the

TABLE I: Description of the random variables used in our model

Symbol	Definition
m	Environmental map
x_t	Self-position of the robot (state variable)
u_t	Control data (action variable)
z_t	Depth sensor data
o_t	Optimality variable (event-driven)
D_e	Duration length for o_t in i_e
i_e	Index of the position distributions
C_e	Index of spatial concepts
f_e	Visual features of the camera image
y_e	Speech signal of the uttered sentence
S_e	Word sequence in the uttered sentence
μ_k, Σ_k	Parameters of multivariate Gaussian distribution (position distribution)
ψ_k	Parameter of the state-transition probability for i_e
π	Parameter of multinomial distribution for C_e
ϕ_l	Parameter of multinomial distribution for i_e
θ_l	Parameter of multinomial distribution for f_e
W_l	Parameter of multinomial distribution for S_e
LM	Language model
AM	Acoustic model for speech recognition
$\alpha, \beta, \gamma, \chi, \omega, \lambda, \lambda, m_0, \kappa_0, V_0, \nu_0$	Hyperparameters of prior distributions

motion of the robot. Because the utterance is event-driven, it is assumed that the variables on the spatial concepts are observed only at event e . The HSMM connects the two units of time and event. Here, T is the last time the robot operated and E is the number uttered by the user or the number of switched places. Let $E < T$ and D_e be the event duration length for e , that is, $T = \sum_{e=1}^E D_e$.

The probability distribution in Eq. (11) can be defined by

unigram rescaling [22], as follows:

$$p(S_e | C_e, W, LM) \stackrel{\text{UR}}{\propto} p(S_e | LM) \prod_{B_e} \frac{\text{Mult}(S_{e,b} | W_{C_e})}{\sum_{c'} \text{Mult}(S_{e,b} | W_{c'})}, \quad (19)$$

where B_e denotes the number of words in the sentence and $S_{t,b}$ is the b -th word in the sentence at time step t .

The probability distribution in Eq. (12) can be defined by unigram rescaling, as follows:

$$p(i_e | C_e, \phi, \psi_{i_{e-1}}) \stackrel{\text{UR}}{\propto} \text{Mult}(i_e | \psi_{i_{e-1}}) \frac{\text{Mult}(i_e | \phi_{C_e})}{\sum_{c'} \text{Mult}(i_e | \phi_{c'})}. \quad (20)$$

The probability distribution in Eq. (14) represents a motion model, that is a state-transition model, in SLAM. The probability distribution in Eq. (15) represents the measurement model in SLAM.

The probability distribution in Eq. (16) can be defined as

$$p(o_t = 1 | x_t, i_e, \mu, \Sigma) = \mathcal{N}(x_t | \mu_{i_e}, \Sigma_{i_e}), \quad (21)$$

where $o_t = 1$ denotes that the event occurred at time t . A binary random variable that indicates whether there is an event is defined as o_t . This event-driven variable corresponds to the optimality variable in the CaI [5].

B. Spatial concept formation

In formulating SpCoTMHP, we describe the joint posterior distribution as

$$x_{0:T}, \mathbf{C}_{1:E}, \Theta \sim p(x_{0:T}, \mathbf{C}_{1:E}, \Theta | u_{1:T}, z_{1:T}, o_{t'_{1:E}}^*, y_{1:E}, f_{1:E}, AM, \mathbf{h}), \quad (22)$$

where the set of latent variables $\mathbf{C}_{1:E} = \{i_{1:E}, C_{1:E}, S_{1:E}\}$, the set of global parameters of the model $\Theta = \{m, \mu, \Sigma, \psi, \pi, \phi, \theta, W, LM\}$ and the set of hyperparameters is denoted by $\mathbf{h} = \{\alpha, \beta, \gamma, \chi, \omega, \lambda, m_0, \kappa_0, V_0, \nu_0\}$. The set of event-driven variables is $o_{t'_{1:E}}^* = \{o_{t'_e} = 1\}_{e=1}^E$.

The variables of the joint posterior distribution can be learned by using Gibbs sampling. Online learning is also possible with particle filters as in SpCoSLAM [3]. Using the Dirichlet process, the number of spatial concepts L and the number of position distributions K were automatically determined according to the data.

In learning, the time of the e -th event (assumed to be the time when the place is indicated by the utterance) is t'_e . Differently expressed, $o_{t'_e} = 1$ is observed at times t'_e , and o_t is unobserved at other times. Therefore, the inference for learning i_e is equivalent to that for an HMM.

Reverse replay: In the case of spatial movement, we can transition from i_{e-1} to i_e and vice versa. Therefore, $i'_{E:1}$, which is replayed using the steps of e in reverse order, can also be used for learning when sampling ψ . This was inspired by the replay performed in the hippocampus of the brain [23].

C. Formulation of path planning by control as inference

The probabilistic distribution, representing trajectory $\tau = \{u_{1:T}, x_{1:T}\}$ when a speech instruction y_e is given, is maximized to estimate an action sequence $u_{1:T}$ (and the path $x_{1:T}$ on the map) as follows:

$$u_{1:T} = \underset{u_{1:T}}{\operatorname{argmax}} p(\tau | o_{1:T}^*, y_{1:E}, x_0, \Theta). \quad (23)$$

The planning horizon at metric level T is the final time of the entire task when one time-step traverses one grid block on the metric map. The planning horizon at topological level E is the number of event steps in the task of navigating by speech instruction. As shown in Eq. (16)–(18), each event step e corresponds to time series $t_e : t'_e$. D_e is the metric-level planning horizon in step e , which corresponds to the duration of the HSMM. In the metric-level planning horizon, the event-driven variable is always $o_{1:T}^* = \{o_t = 1\}_{t=1}^T$ by the CaI. Speech instruction y_e is assumed to be the same as that from $e = 1$ to E . This means that o_t and y_e are multiple optimalities in terms of CaI [24].

From the above, Eq. (23) is as follows:

$$p(\tau | o_{1:T}^*, y_{1:E}, x_0, \Theta) \approx \sum_{C_e} \left[\prod_{e=1}^E \frac{\text{Mult}(i_e | \psi_{i_{e-1}})}{\sum_{c'} \text{Mult}(i_e | \phi_{c'})} \right. \\ \left. \sum_{C_e} \text{Mult}(i_e | \phi_{C_e}) \text{Mult}(S_e | W_{C_e}) \text{Mult}(C_e | \pi) \right. \\ \left. \prod_{t=t_e}^{t'_e} \mathcal{N}(x_t | \mu_{i_e}, \Sigma_{i_e}) p(x_t | m) p(x_t | x_{t-1}, u_e) \right], \quad (24)$$

where $p(x_t | m)$ is a probabilistic representation of the cost map. In this case, we assume that a certain value of $D_{1:E}$ is given. In addition, the word sequence S_e was obtained by speech recognition of y_e . The assumptions, for example, the SLAM models and cost map, in the derivation of the equation are the same as those in [4].

In this study, we assumed that the robot can extract words that indicate the goal and waypoint from a particular utterance sentence. In topological-level planning, including the waypoint, the waypoint word is input in the first half and the goal word in the second half.

D. Approximate inference for hierarchical path planning

Considering the strict inference of Eq. (24), a double-forward backward calculation was executed. In this case, it is necessary to reduce the calculation cost to accelerate path planning, which is one of the purposes of this study. Therefore, we propose an algorithm to solve Eq. (24): Algorithm 1 shows the hierarchical planning algorithm produced by SpCoTMHP.

The concept is that path planning is divided into topological and metric levels, and the CaI is solved at each level. Metric-level planning assumes that the partial paths in each transition between places are solved in A^* . The partial paths can be precomputed regardless of the speech instruction. Topological-level planning is approximated concerning the

Algorithm 1 Hierarchical path planning algorithm.

```

1: // Pre-calculation:
2:  $\{\hat{x}_{t_e|i_e}\} \sim \text{Gaussian\_Mixture}(\phi, \mu, \Sigma)$ 
3: Create a graph between waypoint candidates
4: for all nodes,  $n_{i_{e-1}} \rightarrow n_{i_e}$ , do
5:    $\hat{x}_{i_{e-1}, i_e}^{[n_{i_{e-1}}, n_{i_e}]} \leftarrow \text{A}^*(\hat{x}_{t_{e-1}|i_{e-1}}^{[n_{i_{e-1}}]}, \hat{x}_{t_e|i_e}^{[n_{i_e}]}, w_e)$ 
6:   Calculate likelihood  $\hat{w}_{i_{e-1}, i_e}^{[n_{i_{e-1}}, n_{i_e}]}$  for partial paths
7: end for
8: // When a speech instruction  $y_e$  is given:
9:  $S_e \leftarrow \text{Speech\_Recognition}(y_e, LM, AM)$ 
10: Estimate an index  $i_0$  of the place in initial position  $x_0$ 
11:  $\mathbf{n}_{1:E}, i_{1:E} \leftarrow \text{Search}(i_0, S_e, \hat{w}, \Theta)$  // Eq. (27)
12: Connect the partial paths  $\mathbf{n}_{1:E}$  as the whole path  $\mathbf{x}_{1:E}$ 
13:  $\mathbf{x}_{1:E} \leftarrow \text{Path\_Smoothing}(\mathbf{x}_{1:E}, m)$  // optional process

```

probability distribution of i_e , assuming Markov transitions. Finally, the partial paths in each transition between places are integrated as a whole path. The metric and topological planning can influence each other.

Path planning at the metric level (i.e., partial path $\mathbf{x}_{i_{e-1}, i_e}$ when transitioning from i_{e-1} to i_e) is described as follows:

$$x_{t_e:t'_e} = \underset{x_{t_e:t'_e}}{\text{argmax}} \prod_{t=t_e}^{t'_e} \mathcal{N}(x_t | \mu_{i_e}, \Sigma_{i_e}) \\ p(x_t | m) p(x_t | x_{t-1}, u_e). \quad (25)$$

This means that the inference of a metric-level path can be expressed in terms of CaI.

It was difficult to calculate Eq. (24) for all possible positions. Therefore, we use the mean or sampled values from the Gaussian mixture of position distributions as a goal position candidate, i.e., $i_e \sim \text{Mult}(i_e | \phi)$, and $\hat{x}_{t'_e|i_e}^{[n_{i_e}]} \sim \mathcal{N}(x_t | \mu_{i_e}, \Sigma_{i_e})$. In this case, n_{i_e} is an index that takes values of up to N_{i_e} and the number of candidate points sampled for a certain i_e . By sampling multiple points according to the Gaussian distribution, candidate waypoints that follow the rough shape of the place can be selected. For example, it does not necessarily have to go to the center of a long corridor.

Therefore, as a concrete solution to Eq. (25), the partial path in the transition of candidate points from place i_{e-1} to place i_e is estimated as

$$\hat{x}_{i_{e-1}, i_e}^{[n_{i_{e-1}}, n_{i_e}]} = \text{A}^*(\hat{x}_{t_{e-1}|i_{e-1}}^{[n_{i_{e-1}}]}, \hat{x}_{t'_e|i_e}^{[n_{i_e}]}, w_e), \quad (26)$$

where $\text{A}^*(s, g, w)$ denotes the function of the A^* search algorithm, s is the initial position, g is the goal position, and w is the cost function. Here, $w_e = \mathcal{N}(x_t | \mu_{i_e}, \Sigma_{i_e}) p(x_t | m)$. The estimated partial path length can be interpreted as the estimated value of D_e .

The selection of a series of partial metric path candidates corresponds to the selection of the entire path. Thus, we can replace the formulation of the maximization problem. Each partial metric path has corresponding indices i_{e-1} and i_e . Therefore, if a series of pairs of indices that represent

transitions between position distributions is given, the candidate paths to be considered are naturally narrowed down to the corresponding series of partial paths. The series of candidate indices that determines the series of candidate paths in this case is $\mathbf{n}_{1:E} = (n_{i_0}, n_{i_1}, \dots, n_{i_E})$. This partial path sequence can be regarded as a sampling approximation of $x_{1:T}$.

By taking the maximum value instead of the summing for $i_{1:E}$, path planning at the topological level, is described as

$$\mathbf{n}_{1:E}, i_{1:E} = \underset{\mathbf{n}_{1:E}, i_{1:E}}{\text{argmax}} \prod_{e=1}^E \frac{\text{Mult}(i_e | \psi_{i_{e-1}})}{\sum_{c'} \text{Mult}(i_e | \phi_{c'})} \hat{w}_{i_{e-1}, i_e}^{[n_{i_{e-1}}, n_{i_e}]} \\ \sum_{C_e} \text{Mult}(i_e | \phi_{C_e}) \text{Mult}(S_e | W_{C_e}) \text{Mult}(C_e | \pi), \quad (27)$$

where $\hat{w}_{i_{e-1}, i_e}^{[n_{i_{e-1}}, n_{i_e}]}$ is the likelihood of the metric path $\hat{x}_{i_{e-1}, i_e}^{[n_{i_{e-1}}, n_{i_e}]}$ when the transition from a candidate point of place i_{e-1} to a candidate point of place i_e at step e . In this case, it is equivalent to formulating the state variables in the distribution for the CaI as $\mathbf{x}_{1:E}$ and $i_{1:E}$. Therefore, path planning at the topological level can be expressed as CaI at event step e .

IV. EXPERIMENT I: PLANNING TASKS IN SIMULATOR

We experimented with path planning using spatial concepts including topological structures from human speech instructions. We show that the proposed method can improve the efficiency of path planning. The simulator environment was SIGVerse, version 3.0 [25]. The virtual robot model in SIGVerse is the Toyota Human Support Robot (HSR). We used five three-bedroom home environments² with different layouts and room sizes.

A. Spatial concept-based topometric semantic map

There were 11 spatial concepts and position distributions for each environment. Fifteen training data samples were provided for each location. The SLAM and speech recognition modules were inferred individually by splitting from the model, that is, the self-location $x_{1:E}$ and word sequence $S_{1:E}$ were input to the model as observations. The robot performs SLAM to generate an environment map using the *gmapping* package in the robot operating system (ROS). A word dictionary was provided in advance. We assumed that the speech recognition result was obtained accurately. Model parameters for the spatial concept were obtained via sampling from conditional distribution. We adopted the ideal learning results of spatial concepts, that is, the latent variables C_t and i_t were accurately obtained. Figure 3 shows the example of the spatial concepts.

B. Path planning from speech instructions

The experiment performs two types of path planning tasks. **Basic task:** The robot obtains the word that identifies the target location as the instruction such as ‘*Go to the bedroom*’.

²3D home environment models are available at https://github.com/a-taniguchi/SweetHome3D_rooms.



Fig. 3: Overhead view of the simulator and the spatial concepts expressed by SpCoTMHP on the map. The colors were randomly set. Depending on the transition probability, the center of each Gaussian distribution is connected to an edge.

Advanced task: The robot obtains the words that identify the locations of the waypoint and target as the speech instruction such as ‘*Go to the bedroom via the corridor.*’ Because the task was not demonstrated in [4], both the waypoint and target words were input as bag-of-words into SpCoNavi.

We compare the performances of the methods as follows:

- (A) SpCoSLAM + SpCoNavi (Viterbi)
- (B) SpCoSLAM + SpCoNavi (A* approx.)
- (C) Baseline methods 1 / 2 (Heuristic hierarchical path planning using spatial concepts): Goal position is estimated by $i_e \sim p(i_e | S_e, \Theta)$. The topological planning uses the cumulative cost of a partial path in A* / the partial path distance, instead of Eq. (27).
- (D) SpCoTMHP (Topological: Dijkstra, Metric: A*)

The evaluation metrics for path planning are the success rate (SR), path length (PL), success weighted by path length (SPL) [26], and calculation runtime seconds (Time). The N-SR is the ratio at which the robot reaches its closest location from the initial position when several places have the same name. The W-SR is the ratio of correct waypoints that have been passed. For the evaluation, we corrected the position within the rectangular area surrounding the position coordinates provided by the same place name.

Condition: The planning horizons were $E = 10$ for the topological level and $D = 100$ for the metric level in the SpCoTMHP. The number of position candidates in the sample were $N_{i_e} = 1$. The planning horizon of SpCoNavi was $T = 200$. The number of goal candidates of SpCoNavi (A* approx.) was $J = 1, 10$. The global cost map was obtained from the *costmap_2d* package for the ROS. The robot’s initial position was set from arbitrary movable coordinates on the map. The user provided a word to indicate the target’s name. The state of self-position x_t is expressed discretely for each movable cell in the occupancy grid map m . The motion model assumes a deterministic model. The control value u_t is assumed to move one cell from its current position on

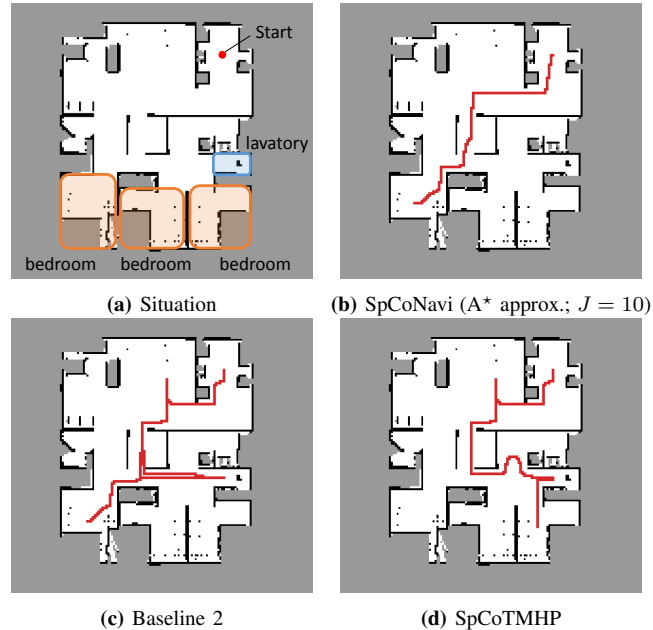


Fig. 4: Example of path planning result in the advanced task. The speech instruction is ‘*Go to the bedroom via the lavatory.*’ (Experiments I).

the map per time-step. Action u_t is discretized into $\mathcal{A} = \{\text{stay, up, down, left, right}\}$. The CPU was an Intel Core i7-6850K with 16GB DDR4 2133MHz SDRAM.

Result: Table II shows the evaluation results for the basic and advanced planning tasks. Figure 4 shows the example of the estimated path. Overall, the evaluation value of the proposed method is better than that of the comparative method, and the calculation time can be significantly reduced compared to SoCoNavi, which requires pre-calculation. For validation, this study was implemented on one CPU using Python, however, the computation time will be further accelerated by parallel processing and the use of GPUs. In the basic task, this also demonstrates that the proposed method solves the problem of stopping the path before reaching the objective, which occurs in SpCoNavi (A* approx.). The N-SR of the baseline methods was lower than that of the proposed method because there were cases where the goal was chosen to be a bedroom far from the initial position. This demonstrated the effectiveness of the proposed method based on the theory of probabilistic inference.

The advanced task confirmed that the proposed method could estimate the path using the waypoint. In contrast, SpCoNavi and baselines could not estimate the path using the waypoint (Fig. 4b). Although the PL of the proposed method tended to be longer than that of others, the reason for this comes from passing through the correct waypoint. The PL could be further shortened by increasing the number of waypoint candidates and adding post-processing to smooth the path. Consequently, the proposed method achieves better path planning by considering all the initial, waypoint, and goal positions.

TABLE II: Evaluation results of the path planning tasks (Experiments I).

Methods	Basic task				Advanced task					
	N-SR↑	PL↓	SPL↑	Time↓	SR↑	N-SR↑	W-SR↑	PL↓	SPL↑	Time↓
SpCoNavi (Viterbi)	0.969	81.5	0.976	2.68×10^3	—	—	—	—	—	—
SpCoNavi (A* approx.; $J = 1$)	0.477	93.5	0.570	9.47×10^0	0.315	0.233	0.455	96.3	0.312	9.44×10^0
SpCoNavi (A* approx.; $J = 10$)	0.389	65.7	0.404	5.42×10^1	0.266	0.252	0.308	59.7	0.266	5.53×10^1
Baseline 1 (partial path cost)	0.750	120.8	0.723	7.56×10^0	0.937	0.784	0.260	121.5	0.917	7.53×10^0
Baseline 2 (partial path distance)	0.710	121.2	0.714	7.96×10^0	0.923	0.736	0.263	121.9	0.902	8.03×10^0
SpCoTMHP	0.941	112.1	0.810	4.79×10^0	1.000	0.860	1.000	186.9	0.881	3.84×10^{-1}

TABLE III: Evaluation results of learning the spatial concept (Experiment II).

Methods	NMI		ARI	
	C_e	i_e	C_e	i_e
SpCoSLAM	0.767	0.803	0.539	0.578
SpCoTMHP	0.779	0.858	0.540	0.656
SpCoTMHP (with reverse replay)	0.786	0.862	0.562	0.658

V. EXPERIMENT II: REAL ENVIRONMENT

We demonstrate that the formation of spatial concepts, including the topological relations of places, can be realized in a real environment. Additionally, we confirmed that the proposed method can plan a path based on the learned topometric semantic map.

A. Spatial concept-based topometric semantic mapping

Condition: The experimental environment was identical to that of the open dataset albert-b-laser-vision, which was obtained from the robotics dataset repository (Radish) [27]. The utterance is 70 sentences such as ‘*This is a dining room*.’ The latent variables including C_t and i_t are estimated by Gibbs sampling. A direct assignment sampler is used to estimate the Markov transition of i_e . The hyperparameters for learning were set as follows: $\alpha = 0.5$, $\gamma = 0.05$, $\beta = 0.1$, $\chi = 1.0$, $m_0 = [0, 0]^T$, $\kappa_0 = 0.001$, $V_0 = \text{diag}(2, 2)$, and $\nu_0 = 3$. The other settings are the same as in Experiment I.

Normalized mutual information (NMI) and adjusted Rand index (ARI), which are the most widely used in clustering tasks for unsupervised learning, were used as the evaluation metrics for learning the spatial concept. NMI is obtained by normalizing the mutual information between the clustering result and the correct label, in the 0.0-1.0 range. ARI is 1.0 when the clustering result matches the correct label and 0.0 when it is random.

Result: Figure 5 shows an example of learning the spatial concept. Table III shows the results of evaluating the average values of 10 trials of learning the spatial concept. SpCoTMHP showed a higher learning performance than SpCoSLAM. In addition, the proposed method with reverse replay had the highest performance. For example, Fig. 5 (b) caused overlapping distributions in the upper right and skipped connections to neighboring distributions, whereas (c) mitigated these problems. As a result, it can be said that using place transitions during learning and vice versa is effective for learning spatial concepts.

B. Path planning from speech instructions

The speech instruction is ‘*Go to the break room via the white shelf*.’ The other settings are the same as in Experiment I. Figure 6 shows the results for path planning using the spatial concept learned in Fig. 5. While SpCoSLAM could not reach the waypoint and goal, SpCoTMHP could estimate the path to reach the goal via the waypoint. The learning with reverse replay in (c) shortened the extra route that would result from the bias of the transition between places during learning in (b). The results show that the proposed method can perform hierarchical path planning accurately, although the learning results are not perfect, as shown in Table III.

VI. CONCLUSIONS

We realized topometric semantic mapping and hierarchical path planning with place-transition patterns based on multimodal observations by robots. Experiments showed that performance in spatial concept formation and path planning improved in simulators and real environments.

Future work will include combining the proposed method with syntactic analysis methods and transferring knowledge of adjacencies between places in multiple environments. The method can also be applied to online path planning, such as model predictive control because the proposed method has become computationally efficient. Additionally, the proposed model has the potential to enable visual navigation and linguistic path explanation tasks through cross-modal inference.

REFERENCES

- [1] I. Kostavelis and A. Gasteratos, “Semantic mapping for mobile robotics tasks: A survey,” *Robotics and Autonomous Systems*, vol. 66, pp. 86–103, 2015.
- [2] S. Garg, N. Sünderhauf, F. Dayoub, D. Morrison, A. Cosgun, G. Carneiro, Q. Wu, T.-J. Chin, I. Reid, S. Gould, P. Corke, and M. Milford, “Semantics for Robotic Mapping, Perception and Interaction: A Survey,” *Foundations and Trends® in Robotics*, vol. 8, no. 1–2, pp. 1–224, 2020.
- [3] A. Taniguchi, Y. Hagiwara, T. Taniguchi, and T. Inamura, “Online Spatial Concept and Lexical Acquisition with Simultaneous Localization and Mapping,” in *IEEE/RSJ International Conference on Intelligent Robots and Systems (IROS)*, 2017, pp. 811–818.
- [4] —, “Spatial Concept-Based Navigation with Human Speech Instructions via Probabilistic Inference on Bayesian Generative Model,” *Advanced Robotics*, vol. 34, no. 19, pp. 1213–1228, sep 2020.
- [5] S. Levine, “Reinforcement Learning and Control as Probabilistic Inference: Tutorial and Review,” *arXiv preprint arXiv:1805.00909*, 2018.
- [6] K. Zheng, A. Pronobis, and R. P. N. Rao, “Learning Graph-Structured Sum-Product Networks for Probabilistic Semantic Maps,” in *AAAI Conference on Artificial Intelligence (AAAI)*, 2018.

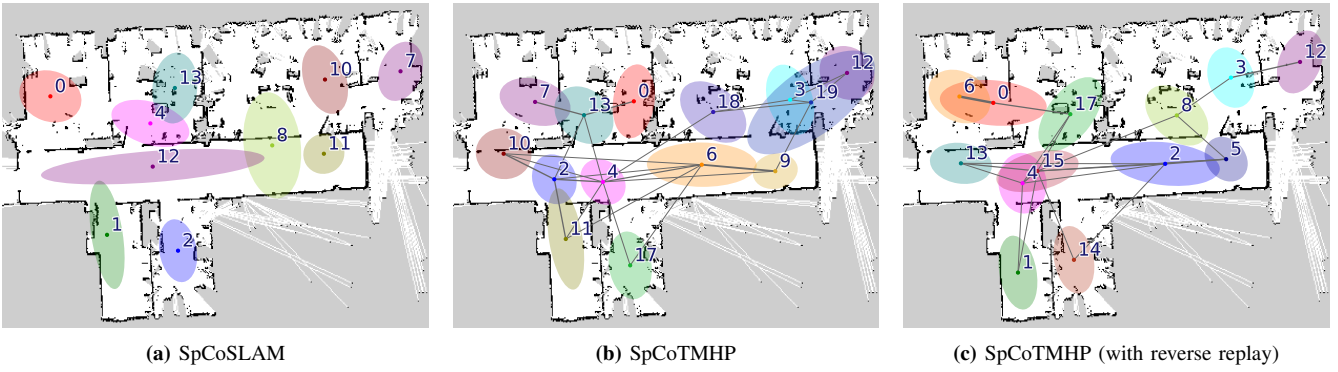


Fig. 5: Result of the spatial concept learning (Experiment II).

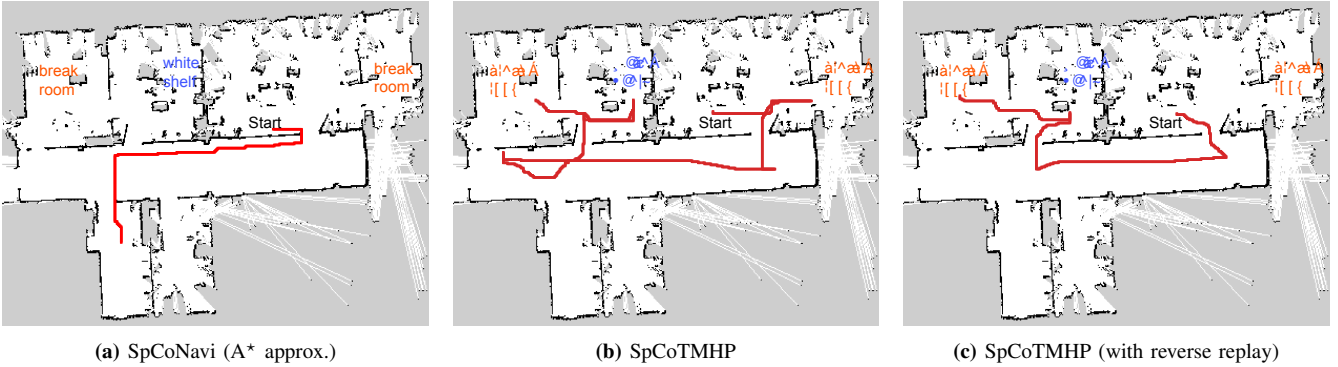


Fig. 6: Result of path planning. The speech instruction is ‘*Go to the break room via the white shelf.*’ The *break room* was taught in two rooms, the upper right and the upper left. The *white shelf* is in the second room from the left on the upper side. (Experiment II).

- [7] I. Kostavelis, K. Charalampous, A. Gasteratos, and J. K. Tsotsos, “Robot navigation via spatial and temporal coherent semantic maps,” *Engineering Applications of Artificial Intelligence*, vol. 48, pp. 173–187, 2016.
- [8] C. Gomez, M. Fehr, A. Millane, A. C. Hernandez, J. Nieto, R. Barber, and R. Siegwart, “Hybrid Topological and 3D Dense Mapping through Autonomous Exploration for Large Indoor Environments,” in *IEEE International Conference on Robotics and Automation (ICRA)*, 2020, pp. 9673–9679.
- [9] A. Rosinol, A. Violette, M. Abate, N. Hughes, Y. Chang, J. Shi, A. Gupta, and L. Carlone, “Kimera: From SLAM to spatial perception with 3D dynamic scene graphs,” *The International Journal of Robotics Research*, vol. 40, pp. 1510–1546, 2021.
- [10] M. Hiller, C. Qiu, F. Particke, C. Hofmann, and J. Thielecke, “Learning Topometric Semantic Maps from Occupancy Grids,” in *IEEE/RSJ International Conference on Intelligent Robots and Systems (IROS)*, 2019, pp. 4190–4197.
- [11] Y. C. N. Sousa and H. F. Bassani, “Topological semantic mapping by consolidation of deep visual features,” *IEEE Robotics and Automation Letters*, vol. 7, no. 2, pp. 4110–4117, 2022.
- [12] L. E. Kavraki, P. Svestka, J.-C. J.-C. Latombe, and M. H. Overmars, “Probabilistic Roadmaps for Path Planning in High-Dimensional Configuration Spaces,” *IEEE Transactions on Robotics and Automation*, vol. 12, no. 4, pp. 566–580, 1996.
- [13] S. M. LaValle, “Rapidly-exploring random trees: A new tool for path planning,” *Research Report 9811*, vol. 98, no. 11, 1998.
- [14] R. C. Holte and M. B. Perez, “Hierarchical A*,” in *AAAI Conference on Artificial Intelligence (AAAI)*, 1996, pp. 530–535.
- [15] G. J. Stein, C. Bradley, V. Preston, and N. Roy, “Enabling Topological Planning with Monocular Vision,” in *IEEE International Conference on Robotics and Automation (ICRA)*, 2020, pp. 1667–1673.
- [16] R. C. Luo and M. Chiou, “Hierarchical Semantic Mapping using Convolutional Neural Networks for Intelligent Service Robotics,” *IEEE Access*, vol. 6, pp. 61287–61294, 2018.
- [17] T. D. Kulkarni, K. R. Narasimhan, A. Saedi, and J. B. Tenenbaum, “Hierarchical deep reinforcement learning: Integrating temporal abstraction and intrinsic motivation,” in *Advances in Neural Information Processing Systems*, 2016, pp. 3682–3690.
- [18] R. Haarnoja, K. Hartikainen, P. Abbeel, and S. Levine, “Latent space policies for hierarchical reinforcement learning,” in *35th International Conference on Machine Learning*, vol. 4, 2018, pp. 2965–2975.
- [19] P. Anderson, Q. Wu, D. Teney, J. Bruce, M. Johnson, N. Sünderhauf, I. Reid, S. Gould, and A. van den Hengel, “Vision-and-language navigation: Interpreting visually-grounded navigation instructions in real environments,” in *IEEE Conference on Computer Vision and Pattern Recognition (CVPR)*, 2018, pp. 3674–3683.
- [20] K. Chen, J. K. Chen, J. Chuang, M. Vázquez, and S. Savarese, “Topological Planning with Transformers for Vision-and-Language Navigation,” in *IEEE Conference on Computer Vision and Pattern Recognition (CVPR)*, 2021, pp. 11271–11281.
- [21] T. Taniguchi, T. Nakamura, M. Suzuki, R. Kuniyasu, K. Hayashi, A. Taniguchi, T. Horii, and T. Nagai, “Neuro-SERKET: Development of Integrative Cognitive System through the Composition of Deep Probabilistic Generative Models,” *New Generation Computing*, vol. 38, pp. 23–48, 2020.
- [22] D. Gildea and T. Hofmann, “Topic-based Language Models Using EM,” in *EUROSPEECH*, 1999.
- [23] D. J. Foster and M. A. Wilson, “Reverse replay of behavioural sequences in hippocampal place cells during the awake state,” *Nature*, vol. 440, no. 7084, pp. 680–683, 2006.
- [24] A. Kinose and T. Taniguchi, “Integration of imitation learning using GAIL and reinforcement learning using task-achievement rewards via probabilistic graphical model,” *Advanced Robotics*, pp. 1–13, 2020.
- [25] T. Inamura and Y. Mizuchi, “SIGVerse: A Cloud-Based VR Platform for Research on Multimodal Human-Robot Interaction,” *Frontiers in Robotics and AI*, vol. 8, p. 158, 2021.
- [26] P. Anderson, A. Chang, D. S. Chaplot, A. Dosovitskiy, S. Gupta, V. Koltun, J. Kosecka, J. Malik, R. Mottaghi, M. Savva, and A. R. Zamir, “On Evaluation of Embodied Navigation Agents,” *arXiv preprint arXiv:1807.06757*, 2018.
- [27] C. Stachniss, “The Robotics Data Set Repository (Radish),” 2003. [Online]. Available: <https://dspace.mit.edu/handle/1721.1/62291>